

Influence of phase quantum fluctuations on superconducting proximity correction in normal-metal wire conductance

Hayato Nakano and Hideaki Takayanagi

NTT Basic Research Laboratories, 3-1 Morinosato-Wakamiya, Atsugi-shi, Kanagawa 243-0198, Japan

(Received 17 December 1999)

The influence of the charging effect on the proximity correction in the conductance of a mesoscopic superconductor(S)/normal-metal(N) coupled system is theoretically investigated. The most important contribution of the proximity correction in the conductance of a diffusive normal metal comes from the correction in the local conductivity $\delta\sigma(r)$. The correction in the conductance is given by $\delta G = (1/L_N^2) \int_{\text{vol}} \delta\sigma(r) dr$. Because of the retro property of Andreev reflection and the long rangeness of the Cooperon (particle-particle ladder), Andreev reflection at the S/N interface affects the local conductivity at a point in the normal region far from the interface (within the phase coherence length L_ϕ). If the S/N interface is very small and has a low transparency, single Andreev reflection is strongly suppressed by the Coulomb blockade at a low temperature ($k_B T < E_C$, $E_C = e^2/2C$) in an exponential manner $\exp\{-4E_C/(k_B T)\}$, where C is the capacitance of the S/N junction. Nevertheless, the proximity correction in the conductance is only suppressed with power law $k_B T/(4E_C)$ because the charged state is an intermediate state in the process of the proximity correction in the conductivity. This is quite different from the charging effect on the proximity correction of the current flowing through the S/N interface, which is strongly suppressed by the charging effect.

I. INTRODUCTION

In the last decade, much attention has been paid to the interference effects in the normal transport in superconductor (S)/normal-metal(N) coupled systems. In such systems the change in a macroscopic phase difference between superconductor electrodes affects the normal transport. This phenomenon is an interference effect of quasiparticles. After the theoretical prediction by Spivak and Khmel'nitskiĭ¹ that such an interference can be observed in weak localization effects in an SN coupled system, Nakano and Takayanagi proposed a model, which is now called the ‘‘Andreev interferometer.’’^{2,3} For Andreev interferometers with diffusive normal metals, recently it has been established that the most important contribution to the interference is different from usual mesoscopic fluctuations, such as weak localizations or universal conductance fluctuations.⁴⁻⁷

On the other hand, the charging effect in a small tunnel junction is one of the most interesting topics in mesoscopic physics.⁸⁻¹⁰ If two metal electrodes are contacted via a very small area interface with a very small capacitance, the charging energy evokes a so-called Coulomb blockade, that is, an exponential suppression of electron transfers through the interface. A perspective description of this charging effect is given by introducing the quantity ‘‘phase’’ (φ), which is the canonical variable to the number of the excess charges (q) that causes a charging energy.

Bruder and co-workers investigated the influence of charging energy on some superconducting proximity effects, such as penetration of the order parameter and magnetic susceptibility in a normal metal attached to a superconductor via a small S/N interface.¹¹⁻¹³ They used a description with the phase variable above. In their description the charging effects on the proximity effects are expressed as results of the quantum fluctuation of the phase. However, they did not in-

vestigate the influence of the fluctuation on the conductance correction because what is the most important contribution to the conductance modulation in SN coupled structures was not clear at that time.

How the ‘‘quantum fluctuation in the phase’’ affects the quasiparticle interferences in Andreev interferometers is a very intriguing question because the phase is the most important quantity in the interferences. As a first step to answering this question, here we investigate the influences of the phase quantum fluctuation on the proximity correction in the normal conductance of a mesoscopic wire attached to a superconductor via a single S/N interface.

According to studies using Keldysh nonequilibrium Green's-function techniques,^{14,15} there are mainly two types of proximity effects on the conductance of an S/N coupled system. One is the renormalization of the tunneling conductance at the S/N interface (i). The other is the correction of the local conductivity in the diffusive normal-metal region (ii).⁴⁻⁶

We will give an explanation of the type-(ii) proximity effect in terms of the Kubo-formula approach of the linear-response theory.¹⁶ This enables us to investigate the charging effects caused at a very small S/N interface on the conductance corrections by using a description of the charging effects that is similar to that by Bruder and co-workers. Huck, Hekking, and Kramer¹⁷ investigated the charging effect on the tunneling current through the S/N interface. At a glance, the situation we consider in this paper might look like their work. However, what they analyzed is the charging effect in the type-(i) proximity effect. We investigate the current that flows only through the normal-metal part. In this case, only the type-(ii) proximity affects the conductance because there is no net tunneling current through the S/N interface. We will show that the charging effect appears in quite a different manner for the type-(i) and type-(ii) proximity effects.

The rest of this paper is organized as follows. In the next section, we give the Kubo-formula approach to the proximity correction in the conductance of a normal-metal wire attached to a superconductor. A brief review of the relation between the fluctuation of the phase and the charging effect in a very small junction is given in Sec. III. Based on the ideas in these two sections, we derive a theory for the influence of the charging effects on the proximity correction in the conductance of mesoscopic normal-metal wires in Sec. IV. In Sec. V, results and discussions are presented.

II. LINEAR-RESPONSE THEORY FOR SUPERCONDUCTING PROXIMITY CORRECTIONS IN THE NORMAL CONDUCTANCE OF A MESOSCOPIC METAL WIRE

Hekking and Nazarov showed that an Andreev interferometer works even if a diffusive normal metal is used.¹⁸ However, the conductance modulation they got was very small because, as described below, two proximity corrections on the local conductivity cancel out each other at the zero-temperature and at the zero-bias voltage limit.^{4,6,18,19} It was established a few years ago from calculations using the Keldysh nonequilibrium Green's-function technique that the conductance modulation in an Andreev interferometer with a diffusive normal-metal region is the modulation of the *average* conductance,^{4,6} which is different from the modulation in the mesoscopic conductance fluctuation predicted by Spivak *et al.* The amplitude of the former can be comparable to the normal conductance without proximity corrections. It is not so clear when this was first pointed out, however, the physics had appeared in early works by Zaitsev and co-workers^{20,21} although they did not emphasize its importance.

Now we know that the conductance modulation in an Andreev interferometer arises from the correction in the local conductivity in the normal region. Here, we will express such a phenomena in terms of the Kubo-formula approach.

A. Local conductivity and conductance

The current density $j(r)$ induced at the point r by an electric field applied at the point r' is given by the Kubo-formula approach of linear-response theory¹⁶ as

$$j(r) = \int_{\text{vol.}} dr' \sigma(r, r') E(r'), \quad (1)$$

where ‘‘vol.’’ means the integration in space over the sample, and

$$\sigma(r, r') = \langle \hat{j}(r) \hat{j}(r') \rangle \quad (2)$$

is the conductivity obtained by the evaluation of the current-current correlation. From Eq. (2), the conductance of a sample is

$$G = \frac{I}{V} = \frac{1}{V^2} \int_{\text{vol.}} \int_{\text{vol.}} dr dr' \sigma(r, r') E(r') E(r), \quad (3)$$

where V is the voltage applied across the sample.

Taking into account the lowest-order correction of impurity scattering, the conductivity can be divided into the local part and nonlocal part,²²

$$\sigma(r, r') = \sigma(r) [\bar{\delta}(r-r') + \nabla_\alpha \nabla'_\beta d(r-r')], \quad (4)$$

where $\bar{\delta}(r-r')$ is a sharply peaked function of the width l , where l is the elastic mean free path due to impurity scatterings. The first term is the local part and the second the nonlocal. The nonlocal part cannot be neglected when the considering the local current conservation. However, by neglecting the mesoscopic correlations in electric fields, we get the ‘‘average’’ conductance,

$$G = \frac{1}{L^2} \int_{\text{vol.}} dr \sigma(r), \quad (5)$$

for a sample that is macroscopically homogeneous in space. Here, L is the sample length. Therefore only the local part of the conductivity contributes to the *average* conductance under these assumptions. This corresponds to taking into account only the contributions that appear in a kinetic equation approach for electronic transports like Boltzmann equation calculation. Equation (5) is valid when the classical electric field is uniform in space. Therefore it is not applicable for a spatially inhomogeneous sample because the electronic field varies with the position and it is not given by $E(r) = E_0 = V/L$. However, we can use

$$\delta G = \frac{1}{L^2} \int_{\text{vol.}} \delta \sigma(r) dr \quad (6)$$

for the correction in conductance δG and in conductivity $\delta \sigma(r)$ if the conductivity without the correction is uniform and the correction is small, that is $|\delta G| \ll |G_0|$, where G_0 is the conductance without proximity correction.

B. Superconducting proximity corrections in local conductivity

The investigations using the Keldysh nonequilibrium Green's-function method have made clear that in diffusive transport cases the most important contribution to the proximity correction in normal conductance comes from the proximity correction in the local conductivity.^{4,5} Here we show the Kubo-formula picture for the corrections.

We consider the system in Fig. 1. This is the simplest geometry for considerations about the proximity corrections in the local conductivity of a mesoscopic metal wire. Although Andreev interferometers have more complicated geometries, the essence of the charging effect on Andreev interferometers already exists in the geometry in Fig. 1, as described in later sections.

In this geometry, there is also a bypass current that flows via the superconductor region. It causes a conductance correction comparable to the correction by the proximity effect, i.e., type (ii). However, here we neglect this bypass current because such a current has nothing to do with the quasiparticle interferences. Actually, we can distinguish the contribution of the proximity correction from the entire conductance by measurement of the magnetoresistance of the geometry in

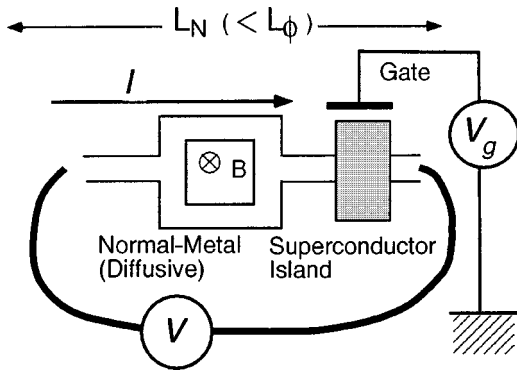


FIG. 1. Normal-metal interferometer with a superconducting island. The ring structure is formed in order to pick up the proximity correction for the whole conductance. A gate is set for detecting the charging effect.

Fig. 1. This is because the proximity correction oscillates with the period in magnetic field corresponding to the flux of $h/2e$.

The normal transport in the normal region is affected by the attached superconductor via Andreev reflections at the S/N interfaces. When an electron (hole) comes to the interface, it is reflected as a hole (electron). Following the notations by Kresin,²³ we express Andreev reflection diagrammatically as shown in Fig. 2.

The normal-metal wire is assumed dirty enough; $\lambda_F \ll l \ll L_N$, where λ_F is the Fermi wavelength in the normal region. In the conductance measurement of the sample, only the type-(ii) proximity effect appears because there is no net current flowing through the S/N interface.

By taking into account the lowest-order corrections due to Andreev reflection, the conductivity with the proximity correction is given by the sums of the contributions of the diagrams in Fig. 3.

The first term (a) gives the conductivity without proximity corrections. The second (b) and third (c) correspond to the diminishment in the conductivity caused by the exclusion of quasiparticle density of states in normal region due to proximity effects. The last term gives a conductivity enhance-

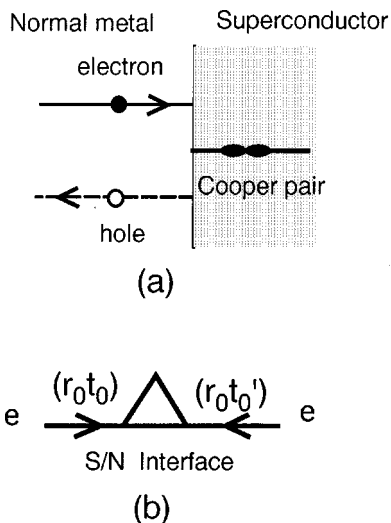


FIG. 2. Andreev reflection at the S/N interface and its diagrammatic expression.

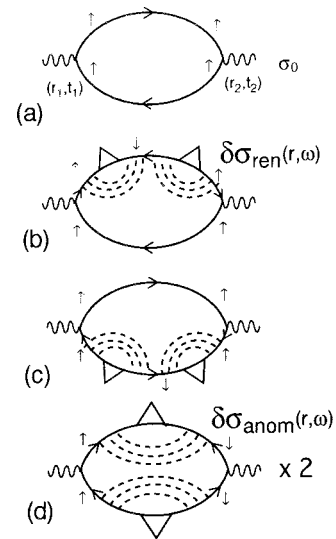


FIG. 3. Perturbation expansion of the proximity correction in the local conductivity $\sigma(r)$. (a) Without perturbation, (b) and (c) conductivity suppressions, and (d) conductivity enhancement. (b) + (c) + (d) = 0 at the absolute zero-temperature and the zero-bias voltage. Arrows show an example of the combination of the spin directions.

ment due to proximity effects. This conductivity enhancement is a Maki-Thompson type of superconducting fluctuation.²⁵ The usual Maki-Thompson effect appears energetically near the superconductivity, that is, just above the superconducting critical temperature. On the other hand, the proximity enhancement here appears spatially near the superconductivity.

It should be noted that the second, the third, and the last terms exactly cancel out each other at the absolute zero-temperature and at the zero-bias voltage limits. Early investigations of proximity correction in conductance by using the Kubo-formula approach²⁴ treated SN systems at such a limit. Therefore the importance of these terms was not emphasized. At a finite temperature or at a finite bias voltage, however, diminishment terms decay with the energy more rapidly than the enhancement term, and the last term exceeds the second and third and gives a large conductance enhancement. The enhancement becomes most significant near the Thouless temperature, $k_B T \sim D/L_N^2$, where D is the diffusion constant in the normal wire. This is the origin of the so-called ‘‘re-entrant behavior,’’ which have been observed recently in experiments.

Andreev reflection forms a two-electron correlation that enhances the conductivity. However, Andreev reflection also decreases the density of states of the single electron. Therefore, in order to consider the superconducting proximity effect, it is very important to take into account self-consistently the modification in the electronic states due to Andreev reflections. This makes diagrammatical perturbation treatments of the proximity correction difficult at a low energy where multiple Andreev reflections are effective. Taking into account the processes in Figs. 3(b)–3(d) at the same time, we can expand the applicable energy of the perturbation calculation.

The rapid decay of the conductivity diminishment with the increase of the energy is explained as follows. In the

propagators with two successive Andreev reflections in Fig. 3(b) or 3(c), a quasiparticle has to traverse two times the round trip from the point $r \sim r_1, r_2$ to the S/N interface. The time for one round trip is of the order of x^2/D , where x is the distance from the S/N interface to the point r . For a point at the end of the wire, the time is the inverse of the Thouless energy E_{Th} . Then, for this process to be effective, the quasiparticle coherence should be kept longer than the $2x^2/D$. At a finite temperature, this gives a decay of $\exp[-\sqrt{k_B T/D}2x]$ to the processes in Fig. 3(b) or 3(c). As a result, the process is effective for the conductivity at point r , which is within region L_T from the S/N interface, where $L_T = \sqrt{D/(k_B T)}$ is the thermal diffusion length.

On the other hand, the enhancement process needs a single round trip. Therefore the diminishment process $\delta\sigma_{\text{ren}}(r)$ needs time reversal symmetry that is two times longer than that needed by the enhancement process $\delta\sigma_{\text{anom}}(r)$. In other words, the diminishment and the enhancement are comparable at a position r within the thermal diffusion length from the S/N interface.

This phenomenon also justifies our taking into account only the lowest- (second-) order Andreev reflection contributions as in Fig. 3. Higher-order contributions include multiple Andreev reflections, or in other words, plural round trips. They are suppressed by a factor like $\exp[-n\sqrt{k_B/D}x]$, where n is the number of round trips. The summation of multiple Andreev reflections is truncated at $n < L_T/x$. Especially at an end of the normal wire, n 's that satisfy $n < \sqrt{E_{Th}}/(k_B T)$ are valid. Very near the S/N interface, higher-order terms should be taken into account. However, at the zero energy limit, the conductivity enhancement and the diminishment cancel each other out at every order and no divergence appears in the perturbation calculation.

It should be noted that the truncation described above is valid for the proximity correction of the conductivity at a point in the normal region. When we consider a current through the S/N interface, multiple Andreev reflections become important because the renormalization of the interface conductance is determined mainly by the electronic states in the vicinity of the S/N interface, those are strongly modified by the multiple Andreev reflections.

In the remainder of this section, for simplicity, we pay attention to the conductivity enhancement term unless stated otherwise. The diminishment term is restored in the result and discussion in Secs. IV and V.

Under the approximation neglecting the nonlocal part of the conductivity, the local conductivity enhancement by the last term in Fig. 3 is given by

$$\delta\sigma(r, \omega) \propto \langle v_F \rangle^2 F_N^R(r, \omega) F_N^A(r, \omega), \quad (7)$$

where $F^{R(A)}$ is the retarded (advanced) anomalous Green's function in the normal region, which is

$$F_N(r, r', t, t') = \lim_{r' \rightarrow r} \langle \psi_{N-\sigma}(r, t) \psi_{N\sigma}(r', t') \rangle, \quad (8)$$

and v_F is the Fermi velocity in the normal region. We can think of the last term of Fig. 3 as corresponding to the classical transport of an extraordinary ‘‘particle’’ whose propa-

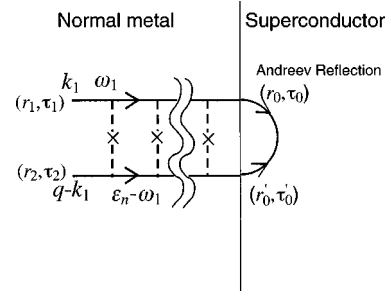


FIG. 4. Anomalous amplitude, $\langle \psi_1(r_1, t_1) \psi_1(r_2, t_2) \rangle$.

gator is the electron-hole correlation of Eq. (8). This result Eq. (7) is the same as that obtained by quasiclassical Keldysh Green's-function approaches.

We emphasize that the $F_N(t_1, t_2, r_1, r_2)$ is not the amplitude of the condensation, or, in other words, the amplitude of a Cooper pair. The condensation amplitude is $\lim_{r_1, t_1 \rightarrow r_2, t_2} [F_N(r_1, r_2, t_1, t_2)]$, which means the probability amplitude where the both electrons exist at the same time at the same position with the precision of $1/\Delta$, the inverse of the superconducting gap energy. The condensation amplitude decreases exponentially with the distance from the superconductor(S)/normal-metal(N) interface by the factor $\exp[-x/L_T]$, as does the conductivity diminishment contribution, where x is the distance from the S/N interface. The condensation carries the nondissipative current, that is, the supercurrent in a thermal equilibrium state, and the ‘‘particle’’ of the propagator carries the dissipative current under a finite applied voltage.

The anomalous Green's functions F_N consist of the particle-particle propagator, the so called ‘‘cooperon,’’²⁶ and Andreev reflection, as illustrated in Fig. 4.^{5,7}

Because of the retro property of Andreev reflection and the long rangeness of the cooperon, this enhancement penetrates into a given point in the normal region far away from the S/N interface within the phase coherence length (L_ϕ). From Fig. 3 and Eqs. (6) and (7), we can roughly estimate the magnitude of the conductance correction as

$$\frac{\delta G}{G_0} \sim \left(\frac{G_T}{G_0} \right)^2, \quad (9)$$

where G_0 is the conductance of the normal-metal wire without proximity corrections, and G_T is the tunneling conductance of the S/N interface when both materials are in the normal state.

Here, it is useful to comment why the impurity corrections taken into account in Fig. 3 are the most important. With respect to proximity correction processes, it is possible to take many kinds of diagrams with different types of vertex corrections. A diagram having vertex corrections for current vertices contributes only when the particle of the ‘‘hole,’’ that is, the upper propagator and the lower propagator in Fig. 3(d), take the same path for the round trip to the S/N interface. As a result, it merely gives a mesoscopic fluctuation in the conductivity. On the other hand, if the vertex corrections for Andreev reflection vertices are taken, as in Fig. 3, the upper and the lower propagator can take paths that are independent to each other. This is not a mesoscopic fluctuation

and gives a large contribution in the conductivity, resulting in a large conductance correction.

III. CHARGING EFFECTS AND QUANTUM FLUCTUATIONS IN THE PHASE OF A SMALL SUPERCONDUCTOR/NORMAL-METAL JUNCTION

Charging effects on the charge transfer across a small tunnel junction were actively researched around 1990.⁹ A perspective description of the effects is given by introducing an operator of called the ‘‘phase.’’ Charging energy evoked by an electron transfer through the junction, causes a time evolution of the phase. The fluctuation in the phase suppresses the charge transfers across the junction and the effect is exactly the same as the phenomenon called the ‘‘Coulomb blockade.’’⁸ The phase is defined by

$$\varphi(t) = \frac{e}{h} \int_{-\infty}^t dt' V(t'), \quad (10)$$

where $V(t)$ is the voltage across the junction. The phase is an operator which works on the excess charge number ‘‘ q ’’ of the junction like

$$e^{i\varphi(t)} q e^{-i\varphi(t)} = q - 2, \quad (11)$$

and satisfies the relation

$$[\varphi, q] = i. \quad (12)$$

An important quantity is the correlation function⁹

$$h(t) = \langle e^{i\varphi(t)} e^{-i\varphi(0)} \rangle. \quad (13)$$

In the case of a small capacitance normal-metal (N)/insulator(I)/normal-metal(N) junction with a highly resistive electromagnetic environment, the tunneling current through the junction is suppressed in the exponential manner $e^{-E_C/(k_B T)}$ if the conditions $k_B T, eV < E_C$, and $G_T < 1/R_Q$ are satisfied by the applied voltage V , temperature T , and tunnel conductance G_T . R_Q is the quantum resistance h/e^2 . This is the Coulomb blockade.

If the applied bias voltage across the junction is zero, the fluctuation in the phase is a quantum fluctuation. According to the description above, we can think of the Coulomb blockade as an obstruction of the charge transfer caused by the ‘‘quantum fluctuation of the phase.’’

The quantum fluctuations in the phase in superconductor (S)/insulator(I)/superconductor(S) tunnel junctions have been intensively investigated in the contexts of macroscopic quantum tunneling, dissipative phase transition, macroscopic quantum coherence, and Bloch oscillations.²⁷ The effective action treatment for the phase variable in $S/I/S$ tunnel junctions gave a transparent view in the analysis of the effect of the quantum fluctuation in the phase. Some people extended the treatment to the analyses of the supercurrent that flows through a superconductor/normal-metal/superconductor ($S/N/S$) system and $S/I/N/I/S$ systems.^{12,28,29}

Bruder and co-workers^{11,12} commented that the estimation of the normal conductance correction with the charging effect is difficult because the spatial dependence should be considered. However, now we know the dominant contribution to the conductance correction is the local conductivity

correction, which changes the average conductance. This makes the analyses of normal conductance corrections much easier. Mesoscopic fluctuations, such as weak localizations and universal conductance fluctuations are sensitive to the sample shape. However, the details of the sample geometry are not important in the local conductivity correction and the resulting correction of *average* conductance due to the proximity effect.

Suppose a normal-metal wire has a superconducting island on it, via an insulator, and this results in a small low-capacitance $S/I/N$ tunnel junction (Fig. 1). This is similar to the model discussed by Bruder and co-workers.^{11,12} The gate electrode on the superconducting island can change the effective charging energy of the S/N junction via control of the average number of excess charges at the junction.

IV. EFFECTS OF THE PHASE QUANTUM FLUCTUATION ON THE TRANSPORT PROPERTY IN A SUPERCONDUCTING PROXIMITY SYSTEM

A. Proximity correction with phase fluctuation

Now we consider the proximity effects induced in the normal-metal region, taking into account the phase dynamics. A finite gate voltage V_g is applied to the superconducting island.

We start from the Hamiltonian of the system described in Appendix A. Following the procedure by Bruder and co-workers, hereafter we use the imaginary time expression for Green’s functions. The proximity effects are treated as the perturbations due to Andreev reflections at the S/N interface.

To emphasize that the charging effect on the proximity correction of the local conductivity, we first briefly consider another superconducting proximity effect, the order-parameter penetration into the normal region. By taking into account the lowest-order contribution of Andreev reflection, the absolute value of the order parameter is calculated like

$$\begin{aligned} |\psi_N(r, \tau_0) \psi_N(r, \tau_0)|^2 &\propto |t|^4 \int_0^\beta d\tau_{01} \int_{A_I} d^2 r_{01} \int_0^\beta d\tau_{02} \int_{A_I} \\ &\times d^2 r_{02} \mathcal{F}_S(r_{02} - r'_{02}, \tau_{02} - \tau'_{02}) \\ &\times \mathcal{F}_S(r'_{01} - r_{01}, \tau'_{01} - \tau_{01}) \\ &\times h_{\text{am}}(\tau_{01}, \tau'_{01}; \tau_{02}, \tau'_{02}) \\ &\times \mathcal{G}_N(r_{01} - r, \tau_{01} - \tau_0) \\ &\times \mathcal{G}_N(r'_{01} - r, \tau'_{01} - \tau_0) \\ &\times \mathcal{G}_N(r - r_{02}, \tau_0 - \tau_{02}) \\ &\times \mathcal{G}_N(r - r'_{02}, \tau_0 - \tau'_{02}), \end{aligned} \quad (14)$$

where \mathcal{G}_N is the normal temperature Green’s function,

$$\mathcal{G}_N(r_2, r_1; \tau_2, \tau_1) = -\langle T_\tau [\psi_{N,\sigma}(r_2, \tau_2) \psi_{N,\sigma}^\dagger(r_1, \tau_1)] \rangle, \quad (15)$$

and \mathcal{F}_S is the anomalous Green’s function in the superconductor region.

$$\mathcal{F}_S(r_2, r_1; \tau_2, \tau_1) = \langle T_\tau [\psi_{S,-\sigma}(r_2, \tau_2) \psi_{S,\sigma}(r_1, \tau_1)] \rangle, \quad (16)$$

$\beta = 1/(k_B T)$, and A_I is the area of the S/N interface. $\langle \dots \rangle_{AV}$ means the quantum-mechanically averaged value in the thermal equilibrium,

$$\begin{aligned} h_{\text{am}}(\tau_{01}, \tau'_{01}; \tau_{02}, \tau'_{02}) &= \left\langle \exp \left\{ \frac{i}{2} [\varphi(\tau_{01}) + \varphi(\tau'_{01})] \right. \right. \\ &\quad \left. \left. - \frac{i}{2} [\varphi(\tau_{02}) + \varphi(\tau'_{02})] \right\} \right\rangle_{AV} \\ &\sim \langle \exp \{ i [\varphi(\tau_{01}) - \varphi(\tau_{02})] \} \rangle_{AV} \\ &\equiv h_{\text{am}}(\tau_{02} - \tau_{01}). \end{aligned} \quad (17)$$

Andreev reflection becomes instantaneous $[\delta(\tau' - \tau)]$ and local in space $[\delta(r' - r)]$ under the conditions

$$eV, k_B T < E_C \ll \Delta. \quad (18)$$

We used this approximation to derive the last expression in Eq. (17). The phase fluctuation caused by the charging effect appears through the correlation function h_{am} in Eq. (17). The correlation function corresponds to the propagator of the energy emission (absorption) of the charging energy to (from) the electromagnetic environment. In this process of the order-parameter penetration, a real energy transfer is needed. Therefore the correlation function gives an exponential suppression in the Coulomb blockade situation.

Similarly, for the excitation of a particle of the propagator $\langle \psi_N(\tau_f) \psi_N(\tau_i) \rangle$, it is necessary that a real energy be emitted to the environment. Therefore if the excitation energy is smaller than the charging energy E_C , the excitation is exponentially suppressed. This makes the propagation of the particle short range in space. When position r is away from the S/N interface by distance x , there is a characteristic time for particle excitation even in the absence of the charging effect. From a rough estimation we get

$$|\tau_0 - \tau_1| \sim |\tau'_0 - \tau'_2| \sim x^2/D \gg \hbar/\Delta \sim |\tau_0 - \tau'_0| \quad (19)$$

for times in the anomalous amplitude in Fig. 4. These time restrictions come from the Green's functions $\mathcal{G}_N(r, \tau)$. When this is combined with the charging effect, we can know that an excitation of the particle should experience the exponential suppression $\exp[-2E_C x^2/D]$ if the excitation energy is smaller than charging energy E_C .

Therefore the penetration of Cooper pairs and induced anomalous amplitude in the normal region are exponentially suppressed by the phase fluctuations. For the supercurrent, which exists in an $SINIS$ geometry, the exponential suppression is inevitable because the carrier of the current, that is, the Cooper pair, is exponentially suppressed by the charging effect, as described above.

Now we proceed to the proximity correction in the electronic transports in the normal region. The simple extrapolation of Eq. (7) in Sec. II to the case under a charging effect gives the conductivity enhancement

$$\delta\sigma \propto \langle \psi_N(r_2, \tau_2) \psi_N(r_1, \tau_1) \rangle \langle \psi_N^\dagger(r_2, \tau_2) \psi_N^\dagger(r_1, \tau_1) \rangle. \quad (20)$$

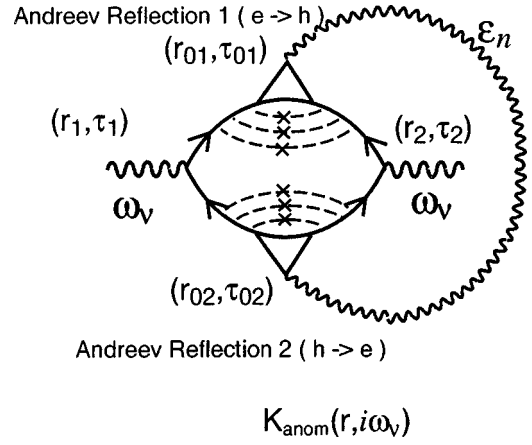


FIG. 5. Proximity conductivity correction with a charging effect.

Since this is the classical product of two particle propagators, it should decrease exponentially due to the charging effect because each propagator in the process is exponentially suppressed as we saw above.

This is not a correct result for the proximity correction in the local conductivity. The electromagnetic response kernel is the two-body-propagator expressed by

$$\begin{aligned} &\langle T_{\tau} [\psi_{N,-\sigma}(r_2, \tau_2) \psi_{N,-\sigma}^\dagger(r_2, \tau_2) \psi_{N,\sigma}(r_1, \tau_1) \psi_{N,\sigma}^\dagger(r_1, \tau_1)] \rangle \\ &\propto |t|^4 \int_0^\beta d\tau_{01} \int_0^\beta d\tau'_{01} \int_0^\beta d\tau_{02} \int_0^\beta d\tau'_{02} \mathcal{G}_N(\tau_{01} - \tau_1) \\ &\quad \times \mathcal{G}_N(-\tau_1 + \tau'_{01}) \mathcal{G}_N(-\tau_{02} + \tau_2) \mathcal{G}_N(-\tau'_{02} + \tau_2) \\ &\quad \times \mathcal{F}_S(\tau_{01} - \tau'_{01}) \mathcal{F}_S(\tau'_{02} - \tau_{02}) \\ &\quad \times h_{\text{tr}}(\tau_{01}, \tau'_{01}; \tau_{02}, \tau'_{02}; \tau_1, \tau_2), \end{aligned} \quad (21)$$

where

$$\begin{aligned} h_{\text{tr}}(\tau_{01}, \tau'_{01}; \tau_{02}, \tau'_{02}; \tau_1, \tau_2) &= \left\langle \exp \left\{ \frac{i}{2} [\varphi(\tau_{01}) + \varphi(\tau'_{01})] \right. \right. \\ &\quad \left. \left. - \frac{i}{2} [\varphi(\tau_{02}) + \varphi(\tau'_{02})] \right\} \right\rangle_{AV} \\ &\sim \langle \exp \{ i [\varphi(\tau_{01}) - \varphi(\tau_{02})] \} \rangle_{AV} \\ &\equiv h_{\text{tr}}(\tau_{02} - \tau_{01}). \end{aligned} \quad (22)$$

To derive this expression, we assumed the condition of Eq. (18). This process is illustrated in Fig. 5.

This becomes more intuitive if we illustrate the image of the term in real space as in Fig. 6. What is most important is as follows. The number of excess charges is the same before the first Andreev reflection at $\tau_{01}(\tau_{02})$ and after the second at $\tau_{02}(\tau_{01})$ because each Andreev reflection causes two-particle tunneling in opposite directions. Therefore $h_{\text{tr}}(\tau_{02} - \tau_{01})$ has a finite expectation value under the average with the unperturbed (without Andreev reflections) states. This is quite different from the order parameter and particle excitation, which has only an exponentially suppressed value under the Coulomb blockade condition.

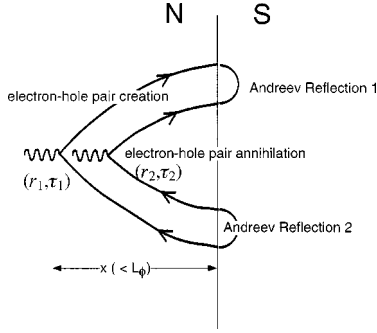


FIG. 6. Image of the conductivity enhancement term in real space.

The lowest-order contribution to the local conductivity enhancement from the kernel in Fig. 5 is given from the linear-response theory as

$$\delta\sigma_{\text{anom}}(\omega, r) = \frac{(v_F \tau_{el})^3 [K_{\text{anom}}(\omega, r) - K_{\text{anom}}(0, r)]}{V_N \omega}, \quad (23)$$

where $\tau_{el} = l/v_F$ is the elastic scattering time, and V_N is the volume of the normal-metal wire. The factor $(v_F \tau_{el})^3/V_N$ appears from the normalization of the function $\bar{\delta}(r-r')$ in Eq. (4).

We can get the proximity correction kernel with the temperature Green's functions,

$$K_{\text{anom}}(i\omega_\nu, r) = \frac{V_N e^2 v_F^2}{h} \sum'_{\omega_l, \varepsilon_n} (k_B T)^2 \text{Re} \left[\mathcal{F}_N \left(r, \omega_l - \omega_\nu + \frac{1}{2} \varepsilon_n \right) \mathcal{F}_N \left(r, \omega_l + \frac{1}{2} \varepsilon_n \right) h_{\text{tr}}(i\varepsilon_n) \right], \quad (24)$$

where Σ' means to take the sum with ω_l 's and ε_n 's that satisfy the conditions $(\omega_l - \omega_\nu)(\omega_l - \omega_\nu - \varepsilon_n) > 0$ and $\omega_l(\omega_l - \varepsilon_n) > 0$. The anomalous Green's function is given by

$$\begin{aligned} \mathcal{F}_N(r, \omega_m) &= \lim_{r_1, r_2 \rightarrow r} \mathcal{F}_N(r_2, r_1, \omega_m) \\ &= \frac{R_Q G_T}{A_I V_N} \left(1 + \frac{|r_1 - r_2|}{l} \text{sgn}[\omega_m] \right) \\ &\quad \times \int_{A_I} dr_0 C_p(r, r_0; \omega_m), \end{aligned} \quad (25)$$

where G_T is the conductance of the interface when both electrodes are in normal states, and A_I is the area of the interface. $C_p(r, r_0; \omega_m)$ is the cooperon (particle-particle ladder), which is the solution of the differential equation

$$\begin{aligned} D(\nabla - 2ie\vec{A})^2 C_p(r, r_0; \omega_m) + (|2\omega_m| + D/L_\phi^2) C_p(r, r_0; \omega_m) \\ = V_N \delta^3(r - r_0), \end{aligned} \quad (26)$$

with the boundary conditions at the S/N interface, at the ends of the wire, and on the side walls of the wire. \vec{A} is the vector potential of the applied magnetic field. Here we took the x axis along the wire. x is the x component of point r . In the

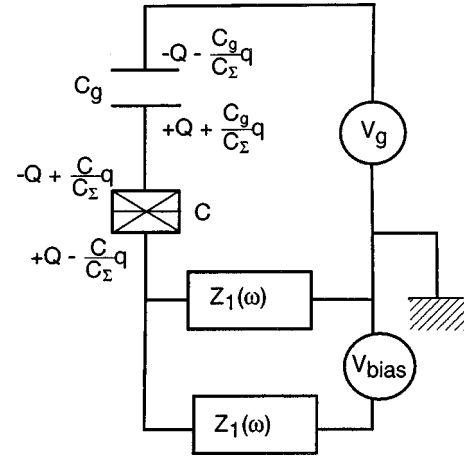


FIG. 7. Effective circuit for the phase motion. $2Z_1(\omega)$ is the impedance of the normal-metal wire without proximity correction.

quasi-one-dimensional case, where the width of the wire is much smaller than the length, the boundary conditions are

$$C_p(r - r_0, \omega_m) \Big|_{r \in x_+, x_-} = 0, \quad (27)$$

where $r \in x_+, x_-$ means that r is at an end of the normal wire.

We can find in Eqs. (24) and (25) that this contribution is classical from the viewpoint of the transport of the particle whose propagator is F_N . The propagator consists of two electrons that travel on the same path to the S/N interface (cooperon). This is finite owing to the mesoscopic effect. However, once the propagator is obtained, the conductivity is determined by the short-range propagation of the particle within the length of the elastic mean free path l . Equation (26) is nothing more than the linearized Usadel equation, which appears in the Keldysh Green's-function analyses for nonequilibrium superconductivities.

By using a calculation similar to that above, we can get the conductivity diminishing contribution of the proximity correction of the second (b) or third (c) term in Fig. 3 with the kernel

$$\begin{aligned} K_{\text{ren}}(i\omega_\nu, r) &= \frac{V_N e^2 v_F^2}{h} \sum'_{\omega_l, \varepsilon_n} (k_B T)^2 \text{Re} \left[\mathcal{F}_N \left(r, \omega_l - \omega_\nu + \frac{1}{2} \varepsilon_n \right) \mathcal{F}_N \left(r, \omega_l - \omega_\nu + \frac{1}{2} \varepsilon_n \right) h_{\text{tr}}(i\varepsilon_n) \right]. \end{aligned} \quad (28)$$

This term corresponds to $F_N^R(r)F_N^R(r) [F_N^A(r)F_N^A(r)]$ of the real-time Green's functions, which decreases with the distance from the S/N interface in an exponential manner like $\exp[-r/L_T]$.

B. Quantum fluctuation of the phase

To estimate the charging effect, we have to analyze the correlation function $h_{\text{tr}}(\tau)$ in Eq. (22). The analysis can be carried out by a calculation similar to that for the usual single electron tunneling conductance. From the viewpoint of the phase motion, the measurement setup in Fig. 1 is converted into the schematic circuit (Fig. 7).

In the setup with a gate electrode, there are two degrees of freedom of charge.³⁰ One is charge Q_g induced across the gate capacitance C_g , the other is Q_c induced across the S/N junction capacitance C . The normal-metal part is the environmental impedance from the viewpoint of the phase motion. The charges are expressed by the island charge q and the continuous charge Q by a canonical transformation;

$$Q_c = Q - \frac{C}{C_\Sigma} q,$$

$$Q_g = -Q - \frac{C_g}{C_\Sigma} q, \quad (29)$$

where $C_\Sigma = C + C_g$. The phases are canonical conjugates of these charges and are given

$$\varphi_- = \varphi - \varphi_g,$$

$$\psi = -\frac{C}{C_\Sigma} \varphi - \frac{C_g}{C_\Sigma} \varphi_g. \quad (30)$$

After some calculations, the correlation function $h_{\text{tr}}(\tau)$ is obtained as

$$h_{\text{tr}}(\tau) = \mathcal{A}_{\varphi_-}(\tau) \mathcal{A}_\psi(\tau), \quad (31)$$

where

$$\mathcal{A}_{\varphi_-}(\tau) = \langle T_\tau e^{i(C_g/C_\Sigma)\varphi_-(\tau)} e^{-i(C_g/C_\Sigma)\varphi_-(0)} \rangle_{\text{env}}$$

$$\equiv \exp \left[\left(\frac{C_g}{C_\Sigma} \right)^2 J_{\varphi_-}(\tau) \right], \quad (32)$$

$$\mathcal{A}_\psi(\tau) = \langle T_\tau e^{-i\psi(\tau)} e^{i\psi(0)} \rangle_{S_{\text{eff}}[\psi]}, \quad (33)$$

$$J_{\varphi_-}(\tau) = \int_0^\infty \frac{d\omega_g}{\omega_g} \frac{\text{Re}[Z_t(\omega_g)]}{R_Q} \left[\coth \left(\frac{1}{2} \beta \omega_g \right) \right. \\ \left. \times [\cosh(\omega_g \tau) - 1] - \sinh(\omega_g |\tau|) \right], \quad (34)$$

$$Z_t(\omega) = \frac{1}{i\omega C_\Sigma + 2/Z_1(\omega)}. \quad (35)$$

In Eq. (33), $\langle \dots \rangle_{S_{\text{eff}}[\psi]}$ means the average is taken by using the effective action $S_{\text{eff}}[\psi]$ of the phase ψ .

The correlation function $h_{\text{tr}}(\tau)$ can be estimated as described in Appendix B. Its Fourier transform is given by

$$h_{\text{tr}}(i\varepsilon_n) = \frac{1 - e^{-4\beta E_C'(V_g)}}{4E_C'(V_g) - i\varepsilon_n}, \quad (36)$$

where $E_C'(V_g)$ is the effective charging energy for the gate controlled S/N junction.

In the derivation, we neglected the friction for the phase fluctuation by ignoring the dissipation for the phase motion due to charge transfer G_A . Therefore we know that Eq. (36) might give an overestimation of the charging effect. In other words, the true influence of the charging effect should be smaller than the one given by Eq. (36). As we will show, the suppression of the proximity corrections by the charging ef-

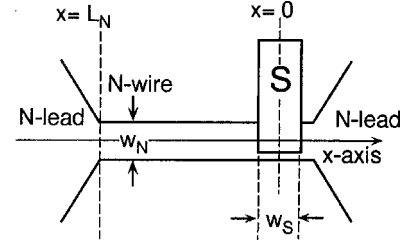


FIG. 8. Quasi-one-dimensional model for calculation.

fect is weak even if we estimate it using the overestimation. Hereafter, we use the simple symbol E_C for the gate controlled effective charging energy instead of $E_C'(V_g)$ because it is clear what it means in the context.

V. RESULTS AND DISCUSSION

A. Proximity correction on the conductance of a normal-metal wire with a single S/N interface

Here we show the results for some concrete models. First, we analyze a simple metal wire with a superconducting island. Suppose the geometry illustrated in Fig. 8. Assuming the wire is much narrower than the phase coherence length L_ϕ , and that the length L_N is much larger than the width, we can take the cooperon as quasi-one-dimensional. Then, Eq. (26) for the cooperon C_p can be solved as

$$C_p(x, \omega_m) = \frac{L_N}{D} \frac{\sinh[\kappa(2\omega_m)(x-L_N)]}{\kappa(2\omega_m) \cosh[\kappa(2\omega_m)L_N]}, \quad (37)$$

where

$$\kappa(\omega_m) = \frac{\sqrt{-\omega_m}}{\sqrt{D}}. \quad (38)$$

From Eqs. (23) and (24), finally we get the correction in the dc conductivity,

$$\delta\sigma_{\text{anom}}(x) = \sigma_0 \frac{1}{D^2} \left(\frac{R_Q G_T}{A_N N_N(0)} \right)^2 \\ \times \int_{-\infty}^{\infty} dz \frac{\partial n_F(E)}{\partial E} \Big|_{E=z} \sum_{n=-\infty}^{\infty} (k_B T) \\ \times \text{Re} \left[\frac{\sinh[\kappa_+(x-L_N)] \sinh[\kappa_-(x-L_N)]}{\kappa_+ \cosh[\kappa_+ L_N] \kappa_- \cosh[\kappa_- L_N]} \right] \\ \times h_{\text{tr}} \left(i \frac{2n\pi}{\beta} \right). \quad (39)$$

Similarly, for the conductivity diminishment contribution,

$$\delta\sigma_{\text{ren}}(x) = \sigma_0 \frac{1}{D^2} \left(\frac{R_Q G_T}{A_N N_N(0)} \right)^2 \int_{-\infty}^{\infty} dz \frac{\partial n_F(E)}{\partial E} \Big|_{E=z} \\ \times \sum_{n=-\infty}^{\infty} (k_B T) \text{Re} \left[\left(\frac{\sinh[\kappa_+(x-L_N)]}{\kappa_+ \cosh[\kappa_+ L_N]} \right)^2 \right] \\ \times h_{\text{tr}} \left(i \frac{2n\pi}{\beta} \right). \quad (40)$$

After the integration over the volume of Eq. (6), the conductance corrections are given by

$$\begin{aligned} \delta G_{\text{anom}} = & \frac{G_T^2}{G_0} \int_{-\infty}^{\infty} dz \frac{\partial n_F(E)}{\partial E} \Big|_{E=z} \sum_{n=-\infty}^{\infty} (k_B T) \\ & \times \text{Re} \left[\frac{2h_{\text{tr}} \left(i \frac{2n\pi}{\beta} \right)}{L_N^3 (\kappa_+ \kappa_-) \cosh[\kappa_+ L_N] \cosh[\kappa_- L_N]} \right. \\ & \left. \times \left\{ \frac{\sinh[(\kappa_+ + \kappa_-) L_N]}{\kappa_+ + \kappa_-} - \frac{\sinh[(\kappa_+ - \kappa_-) L_N]}{\kappa_+ - \kappa_-} \right\} \right]. \end{aligned} \quad (41)$$

Similarly,

$$\begin{aligned} \delta G_{\text{ren}} = & \frac{G_T^2}{G_0} \int_{-\infty}^{\infty} dz \frac{\partial n_F(E)}{\partial E} \Big|_{E=z} \sum_{n=-\infty}^{\infty} (k_B T) \\ & \times \text{Re} \left[\frac{\left(-\frac{1}{2} + \sinh[2\kappa_+ L_N] \right)}{L_N^3 (\kappa_+ \cosh[\kappa_+ L_N])^2} h_{\text{tr}} \left(i \frac{2n\pi}{\beta} \right) \right], \end{aligned} \quad (42)$$

where

$$\kappa_{\pm} = \kappa \left(\pm 2iz - \frac{2|n|\pi}{\beta} \right). \quad (43)$$

Equations (39) and (40) show that the charging effects appear in the proximity corrections of the local conductivity as an exponential cutoff whose characteristic length is on the order of the thermal diffusion length $(D\beta)^{(1/2)}$. Summing up with n , it is clear that at a temperature $k_B T > E_{\text{Th}}$, the contributions of the terms of $n \neq 0$ are infinitesimally small. This is the fact that neither the energy emission to the environment nor the absorption from the environment as a real process is possible at the low temperature. Only the virtual excitation of the environment contributes to the proximity process. Physically, the meaning of this is as follows. An Andreev reflection needs two-particle tunneling through the S/N interface, and the tunneling evokes a charged state in a Coulomb blockade situation. However, in the process in Fig. 6, the charged state can be included as a quantum intermediate state because each two-particle tunneling is in the opposite direction.

This is physically quite different from the Andreev tunneling current through the S/N interface, which was analyzed by Huck, Hekking, and Kramer.¹⁷ In the case of the tunneling current, two electrons should transfer through the S/N interface as a real process. The process needs real energy emission or real energy absorption. In the Coulomb blockade situation, that is, $k_B T, eV < E_C$, such emission and absorption are almost impossible as described above. Therefore the Andreev tunneling current cannot avoid the exponential suppression by the Coulomb blockade.

Contrary to the fact that finite energy z simultaneously gives an exponential decay and sinusoidal oscillation to the spatial dependence of the local conductivity with the dis-

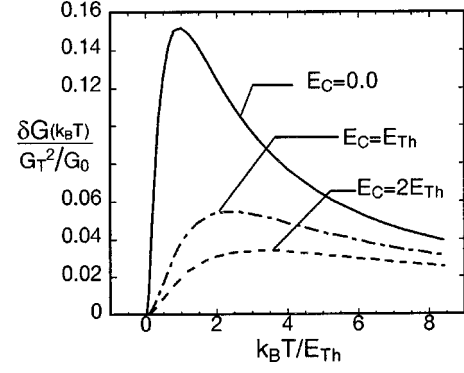


FIG. 9. Calculated temperature dependence of the conductance corrections.

tance from the S/N interface, a term with finite n decays monotonically with the distance. Therefore, the conductivity corrections of a sample that is longer than the thermal diffusion length, the term of $n=0$ dominates, are expected that

$$\frac{\delta\sigma(0,r)}{\delta\sigma(0,r)|_{E_C=0}} \sim \frac{1}{4E_C\beta}. \quad (44)$$

The total conductance correction is $\delta G = \delta G_{\text{anom}} - \delta G_{\text{ren}}$. Equation (44) also suggests:

$$\delta G[E_C, k_B T] \propto \begin{cases} (k_B T)^3 & \text{for } k_B T < E_{\text{Th}}, E_C, \\ \text{const} & \text{for } E_{\text{Th}} < k_B T < E_C, \\ (k_B T)^2 & \text{for } E_C < k_B T < E_{\text{Th}}, \\ (k_B T)^{-1} & \text{for } E_C, E_{\text{Th}} < k_B T. \end{cases} \quad (45)$$

The results of the numerical calculation of the conductance corrections with and without the charging effect, using Eqs. (41) and (42) are shown in Fig. 9.

Figure 10 shows the growth of the conductance corrections from the zero temperature. The curves are plotted with the log-log scale in order to clarify the power of the rise. As the third and first lines in Eq. (45) give, when $E_C = 0$ the correction δG rises with $(k_B T)^2$, and when $E_C = 2E_{\text{Th}}$ it rises with $(k_B T)^3$. When $E_C = 0.1E_{\text{Th}}$, we can see the transition of the power from 3 to 2 near $k_B T \sim E_C = 0.1E_{\text{Th}}$. This means that above the temperature, the conductivity correction process can occur with ‘‘real’’ emission to the environment.

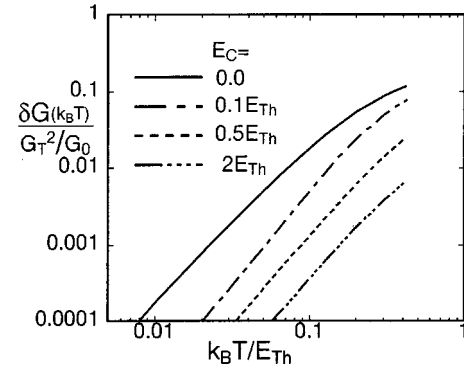


FIG. 10. Growth of the proximity correction at low temperatures for various charging energies.

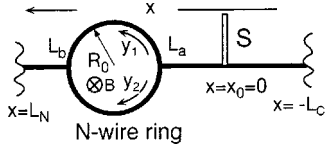


FIG. 11. Quasi-one-dimensional model for the interference.

As a result, in contrast to the Coulomb blockade, which gives exponential suppression $\exp[-4E_C/(k_B T)]$, the charging causes a decrease in the proximity correction in the normal-metal conductance with the power law $k_B T/(4E_C)$. The charging effect does not strongly suppress the proximity correction in the local conductivity and the resulting correction in the conductance δG .

Another explanation for this weak suppression is possible. As can be seen in Fig. 5, the time lag $\tau_{01} - \tau_{02}$ between two Andreev reflections can be shorter than $1/E_C$ because it is possible that, for example,

$$|\tau_{01} - \tau_{02}| \ll |\tau_{01} - \tau_1|, |\tau_{02} - \tau_2|. \quad (46)$$

Therefore, in the proximity correction process, the time during which the system is in the charged state can be much shorter compared to the other proximity effects which have a time constriction like Eq. (19).

B. Phase quantum fluctuation in interferometer

For a real measurement, the calculated model in Fig. 8 is too simple to distinguish the proximity correction from the entire conductance. In order to do that, an interferometer like that in Fig. 1 is necessary. However, the above quantitative discussion of the charging effect for the model is still valid for an interferometer because the interference in the ring structure is quite simple.

Suppose a geometry with a ring, as illustrated in Fig. 11. The ring is pierced by a magnetic field. If we solve differential equation (26) with the boundary conditions for the quasi-one-dimensional interferometer structure illustrated in Fig. 11, we immediately get the cooperon in the structure. The derivation is given in Appendix C. The solutions, Eqs. (C2)–(C4), show that the interference is a simple Aharonov-Bohm-type interference in a single-channel ring, if we imagine the cooperon itself is a particle with the charge $2e$. Now, we focus on the conductance correction in the left part $x_0 < x$ because the correction in the right part $x < x_0$ is not so sensitive to the magnetic field.

More simplification is possible when the temperature is lower than the Thouless energy ($k_B T < E_{Th}$), where now $E_{Th} = D/(L_L + L_R + \pi R_0)^2$. Approximating variables that slightly depend on the geometry as constants, the system with the loop at the low temperature is quantitatively equivalent to the much simpler system illustrated in Fig. 12.

It is a single wire with a transmission controller at position $x = L_b$, where the left node of the loop is. Magnetic flux piercing the loop is taken over by the controller, which modifies the transmission coefficient for the cooperon t_{coop} with the relation

$$t_{coop} = \cos \left[2\pi \frac{\Phi}{\Phi_0} \right], \quad (47)$$

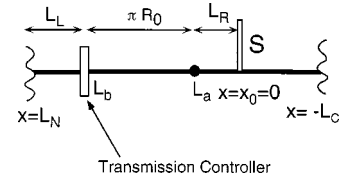


FIG. 12. Equivalent system at a low temperature for the loop geometry in Fig. 11.

where $\Phi_0 = h/e$ is the quantum flux. This simplification is possible because, as discussed in Sec. II, the transport is classic, or ‘‘local,’’ as expressed in the first term of the right-hand side in Eq. (4). The conductivity oscillation due to the interference comes from the oscillation in the propagator of Eqs. (C2)–(C4). In the case of a mesoscopic fluctuation, the interference appears in the correlation between two or more propagators. The interference in the proximity corrections does not come from the mesoscopic ‘‘transport,’’ but from a mesoscopic propagator, which corresponds to the particle.

At the magnetic field corresponding to the flux $\Phi = k\Phi_0/2$, where k is an integer, the anomalous amplitude $F_N(r)$ has a large magnitude even at the left end of the wire ($x = L_N$) because the transmission is unity. On the other hand, for $\Phi = (2k + 1)\Phi_0/4$, F_N is blocked at $x = L_b$ because the transmission is closed. An increase in magnetic field gives the cycle between these ‘‘open’’ and ‘‘close’’ conditions. From the viewpoint of the proximity conductance correction, this cycle corresponds to changing the length of the normal wire between $L_L + L_R + \pi R_0$ and $L_R + \pi R_0$. Therefore the conductance correction oscillates with the period of flux $h/(2e)$ when the magnetic field is increased. Since the conductance correction of a single wire is given from the conductivity corrections in Eqs. (41) and (42), we can estimate the amplitude of the oscillation in the magnetoconductance. Taking care to the fact that the Thouless energy E_{Th} changes with the effective length of the normal region, which now oscillates, and the energy dependence of the correction can be normalized by the Thouless energy, the amplitude is approximately given by

$$A_{osc} \equiv \delta G[\Phi = 0, k_B T] - \delta G[\Phi = \Phi_0/4, k_B T] \\ \sim \delta G[\Phi = 0, k_B T] - \delta G[\Phi = 0, k_B T/r_L^2] r_L, \quad (48)$$

where

$$r_L = \frac{L_L + L_R + \pi R_0}{L_R + \pi R_0}. \quad (49)$$

As discussed for the single-wire geometry, from Eqs. (45) and (48),

$$A_{osc} \sim \delta G[\Phi = 0, k_B T] \begin{cases} (1 - 1/r_L) & \text{for } k_B T < E_{Th}, E_C, \\ [1 - 1/(r_L)^3] & \text{for } E_C < k_B T < E_{Th}. \end{cases} \quad (50)$$

A_{osc} is of the same order of $\delta G(\Phi = 0)$ if $L_L \geq L_R + \pi R_0$.

On the other hand, at a high temperature $E_{Th} < k_B T \ll \Delta$, the most phase-sensitive contribution is the proximity correction of the conductivity in the right lead, and the oscillation is given by

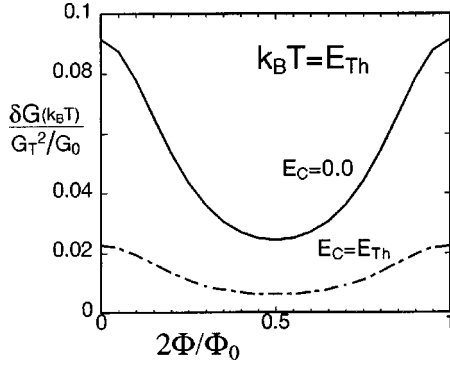


FIG. 13. Numerical calculation for the magnetoconductance oscillation due to the proximity correction in the interferometer in Fig. 11.

$$\delta G(\Phi=0) - \delta G(\Phi) \sim \alpha \frac{E_{Th}}{k_B T} G_1 \sin^2[2\pi\Phi/\Phi_0] \times \exp\left[-\frac{\pi R_0 + L_R}{\pi R_0 + L_R + L_L}\right], \quad (51)$$

where G_1 is a positive value of the order of G_T^2/G_0 , which is insensitive to the flux Φ , and α is 1 for $E_C < E_{Th}$ and $k_B T/E_C$ for $E_C > E_{Th}$. Therefore the amplitude of the magnetoconductance oscillation is estimated as

$$A_{osc} \sim \frac{G_T^2}{G_0} \exp\left[-\frac{\pi R_0 + L_R}{\pi R_0 + L_R + L_L}\right] \times \begin{cases} \frac{D}{L_N^2 k_B T} & \text{for } E_C < E_{Th} < k_B T, \\ \frac{D}{L_N^2 E_C} & \text{for } E_{Th} < k_B T < E_C. \end{cases} \quad (52)$$

The result of the numerical calculation for the interferometer in Fig. 11 using the exact solution in Appendix C is shown in Fig. 13.

It shows that the conductance correction oscillates with the period of $h/(2e)$. The temperature dependences of the oscillation amplitude are shown in Fig. 14.

The influence of the charging effect and the temperature dependence are quite similar to the case of the conductivity

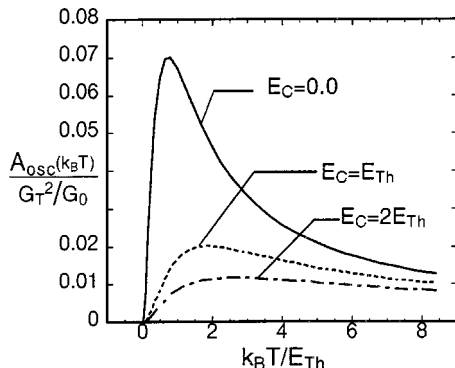


FIG. 14. Numerical calculation for the amplitude of the magnetoconductance oscillation due to the proximity correction in the interferometer in Fig. 11.

correction of the simple wire. This is the most significant manifestation that the proximity correction of the ‘‘average’’ conductance is caused by the ‘‘classical’’ transport of a mesoscopic particle.

C. Charging effect on an Andreev interferometer

Up to this point, we have considered the proximity corrections in the normal region of normal-metal–superconductor coupled systems that have only one S/N interface. Andreev interferometer seems to be more interesting for investigating the proximity corrections because the macroscopic phases appear explicitly in it.

Here, we will briefly discuss the phase fluctuations due the charging effects on an Andreev interferometer, that is, an SN coupled system with plural S/N interfaces.

As described in the previous sections, we are interested in conductance for the current that flows without passing through the S/N interface. For systems with a single S/N interface, the quantum fluctuation of the phase does not strongly destroy the interference effect in the conductance correction due to the proximity effect. This is mainly because the time lag between two Andreev reflections in the process can be small.

If we ignore the environment of the S/N interfaces in Andreev interferometers, that is, if we assume that the superconducting circuit, that determines the macroscopic phase differences, does not affect the charging effect at the S/N interfaces and the macroscopic phases are definite, the extrapolation of the above approach to an Andreev interferometer gives the result that the proximity correction which is sensitive to the macroscopic phase difference of the interferometer is suppressed by the factor $\exp[-2E_C(L_I^2/D)]$, where L_I is the distance between two S/N interfaces. Therefore the sensitivity of the interferometer is strongly dependent on the distance between two S/N interfaces even at a very low temperature.

The above assumption, however, is too naive. If we consider the quantum-mechanical aspects in the macroscopic phase of the Andreev interferometer, we must take into account the quantum-mechanical dynamics of external circuits, for example, an external Josephson junction.³¹ Even if the mechanism which determines the macroscopic phase difference is the same in the sense of classical dynamics of the phase, a difference in the quantum-mechanical aspect can change the proximity correction in the Andreev interferometer. An analysis of the phase fluctuation effects on Andreev interferometers will appear elsewhere.³²

D. Summary

We investigated the influence of the quantum fluctuation on the superconducting proximity correction of the conductivity in a normal-metal mesoscopic wire having a superconducting island on it via a small S/N interface. The charging energy at the interface causes a phase fluctuation. However, contrary to the Coulomb blockade of the tunneling current through the S/N interface, the proximity correction of the conductivity and resulting conductance correction are merely suppressed by the power law.

From the viewpoint of the relation between the quantum fluctuation of the phase and the interference effect, the situ-

ation can be summarized as follows. The charging effect at the S/N interface causes the quantum fluctuation of the phase. However, the fluctuation does not strongly destroy the quasiparticle interference in the proximity conductance correction process because two Andreev reflections in the process can occur in time near each other. Therefore the difference between the two phases the quasiparticles get at the Andreev reflections can be small even if the phase is quantum mechanically fluctuating.

ACKNOWLEDGMENTS

The authors thank Professor D. Averin and Professor G. Schön for their valuable advice. They are also grateful to Dr. Y. Tohkura and S. Ishihara for their encouragement throughout this work.

APPENDIX A: HAMILTONIAN FOR THE CALCULATION

The Hamiltonian of this system is

$$\mathcal{H} = \mathcal{H}_N + \mathcal{H}_S + \mathcal{H}_T + \mathcal{H}_C, \quad (\text{A1})$$

where

$$\begin{aligned} \mathcal{H}_N = & \sum_{\sigma} \int_{\text{vol.N}} \psi_{N,\sigma}^{\dagger}(r) \left(\frac{1}{2m^*} \right) \frac{\partial^2}{\partial r^2} \psi_{N,\sigma}(r) d^3r \\ & + \sum_{\sigma} \int_{\text{vol.N}} V_{\text{imp}}(r) \psi_{N,\sigma}^{\dagger}(r) \psi_{N,\sigma}(r) d^3r \\ & + \sum_{\sigma} \int_{\text{vol.N}} (-\mu_N) \psi_{N,\sigma}^{\dagger}(r) \psi_{N,\sigma}(r) d^3r, \quad (\text{A2}) \end{aligned}$$

$$\begin{aligned} \mathcal{H}_S = & \sum_{\sigma} \int_{\text{vol.S}} \psi_{S,\sigma}^{\dagger}(r) \left(\frac{1}{2m^*} \right) \frac{\partial^2}{\partial r^2} \psi_{S,\sigma}(r) d^3r \\ & + \sum_{\sigma} \int_{\text{vol.S}} [\Delta(r) \psi_{S,\sigma}^{\dagger}(r) \psi_{S,-\sigma}^{\dagger}(r) + \text{H.c.}] d^3r \\ & + \sum_{\sigma} \int_{\text{vol.S}} (-\mu_S) \psi_{S,\sigma}^{\dagger}(r) \psi_{S,\sigma}(r) d^3r, \quad (\text{A3}) \end{aligned}$$

$$\mathcal{H}_T = \sum_{\sigma} \int_{A_I} [t \psi_{S,\sigma}^{\dagger}(r_0) \psi_{N,\sigma}(r_0) + \text{H.c.}] d^2r_0 \quad (\text{A4})$$

$$\mathcal{H}_C = \frac{e^2}{2C} (\tilde{n}_N - \tilde{n}_S - Q_g)^2, \quad (\text{A5})$$

$$\tilde{n}_N = n_N - \langle n_N \rangle, \quad (\text{A6})$$

$$\tilde{n}_S = n_S - \langle n_S \rangle, \quad (\text{A7})$$

$$n_N = \sum_{\sigma} \int_{\text{vol.N}} \psi_{N,\sigma}^{\dagger}(r) \psi_{N,\sigma}(r) d^3r, \quad (\text{A8})$$

$$n_S = \int_{\text{vol.S}} \psi_{S,\sigma}^{\dagger}(r) \psi_{S,\sigma}(r) d^3r. \quad (\text{A9})$$

Here, μ_N is the chemical potential of the normal region, $\tilde{n}_N - \tilde{n}_S$ is the number operator of the excess charge, $Q_g = C_g V_g / e$ is the average number of the excess charges induced by the gate voltage V_g . In this Hamiltonian, the tunneling matrix element t is normalized to express that the electron tunnelings occur only at the S/N interface. We can take a grand canonical ensemble even for a small superconducting island at a finite temperature.

APPENDIX B: ESTIMATION OF THE CORRELATION FUNCTION

Assuming that the impedance of the normal-metal wire is mainly Ohmic, then Eq. (34) becomes

$$\begin{aligned} J_{\varphi_-}(\tau) = & - \int_0^{\infty} d\omega_g \frac{R_N}{4R_Q} \frac{1}{1 + (R_N \omega_g C_{\Sigma}/4)^2} \left[\frac{\tau^2}{\beta} + |\tau| \right] \\ \sim & - \frac{\arctan(C_{\Sigma} R_N \omega_c / 4)}{C_{\Sigma}} \left(|\tau| + \frac{1}{\beta} \tau^2 \right), \quad (\text{B1}) \end{aligned}$$

where $R_N = 1/G_0$ is the dc resistance of the normal-metal wire without the proximity effect. ω_c is an appropriate cutoff frequency which is of the order of the gap energy Δ in the superconducting region. In a realistic case, since $R_N/R_Q \sim 10^{-2} \sim 10^{-3}$, the argument $C_{\Sigma} R_N \Delta$ is smaller than unity. Therefore we get

$$\mathcal{A}_{\varphi_-}(\tau) \sim \exp \left[- \left(\frac{C_g}{C_{\Sigma}} \right)^2 \frac{R_N \Delta}{4R_Q} \left(|\tau| + \frac{1}{\beta} \tau^2 \right) \right] \sim 1. \quad (\text{B2})$$

This means that the fluctuation of the phase for φ_- due to the electromagnetic environment is negligible.

On the other hand, the effective action for the phase motion $\psi(\tau)$ in Eq. (33) is given by

$$\begin{aligned} S_{\text{eff}}[\psi] = & \int_0^{\beta} d\tau \left[\frac{C_{\Sigma}}{2} \frac{1}{2e} \left(\frac{\partial \psi}{\partial \tau} \right)^2 + i n_c \frac{\partial \psi}{\partial \tau} \right] \\ & - \int_0^{\beta} d\tau_{01} \int_0^{\beta} d\tau_{02} \int_{A_I} dr_{01} \int_{A_I} dr_{02} \left(\frac{G_T R_Q}{A_I V_N} \right)^2 \\ & \times C_N(r_{02} - r_{01}, \tau_{02} - \tau_{01}) \cos[\psi(\tau_{02}) - \psi(\tau_{01})], \quad (\text{B3}) \end{aligned}$$

where $C_N(r_{02} - r_{01}, \tau_{02} - \tau_{01})$ is another Cooperon in the normal region which connects two Andreev reflections at points (r_{01}, τ_{01}) and (r_{02}, τ_{02}) . It is given by the solution of Eq. (26) too. The third term in Eq. (B3) expresses the effect of the dissipation due to the fluctuation of the island charge via Andreev reflection tunneling through the S/N interface. Here we assume that the dissipation is ohmic, or in other words, that the Andreev tunneling can be expressed with a parameter G_A , which has a dimension of the conductance and is smaller than G_T .

Paying attention to the fact that we cannot distinguish ψ and $\psi + 2k\pi$, where k is an integer, we get from Eq. (33)

$$A_\psi(\tau) = \sum_{n=-\infty}^{\infty} e^{-4\beta E_C(n-n_c)^2} e^{-4E_C[|\tau|-2(n-n_c)\tau+4G_A R_Q|\tau|]} \times \left(\sum_{n=-\infty}^{\infty} e^{-4\beta E_C(n-n_c)^2} \right)^{-1}, \quad (\text{B4})$$

where n_c is the charge misfit parameter given by

$$en_c = C_g \left(V_g - \frac{1}{2} V_{\text{bias}} \right). \quad (\text{B5})$$

In principle, the charge misfit parameter depends on the bias voltage V_{bias} across the wire. However, in an actual situation, $en_c \sim V_g C_g = eQ_g$ because $V_g \gg V_{\text{bias}}$.

For simplicity, moreover, we consider the case where E_C is very large so that we have to take into account only the $|n-n_c| \leq 1$ states. In this case, Eq. (B4) is much simplified to

$$A_\psi(\tau) = \frac{\cosh[4E_C\beta(n^+ - n_c + 1/2) - 4E_C\tau]}{\cosh[4E_C\beta(n^+ - n_c + 1/2)]} \times e^{-4E_C[|\tau|-2(n^+ - n_c + 1/2)\tau+4G_A R_Q|\tau|]}, \quad (\text{B6})$$

where n^+ is the smallest integer which satisfies $n^+ \geq n_c$. Equation (B6) shows $A_\psi(\tau)$ oscillates as a function of n_c between $e^{-4E_C G_A |\tau|}$ and $e^{-4E_C(\tau + G_A |\tau|)}$. This corresponds to the fact that the effective charging energy of the S/N junction is a function of the gate voltage V_g and we express it as $E'_C(V_g)$. Strictly speaking, since G_A depends on the phase fluctuation, it should be determined self-consistently through the equation.¹⁷

$$G_A = 4R_Q \left(\frac{G_T}{A_I N_N(0)} \right)^2 \lim_{eV \rightarrow 0} \left\{ \frac{1}{V} \text{Im} \left[(k_B T) \times \sum_{\varepsilon_n} \int_{A_I} dr_{01} \int_{A_I} dr_{02} h_{\text{tr}}(i\varepsilon_n) \times C_N(r_{02} - r_{01}, \omega_\nu - \varepsilon_n) \right] \right\}_{i\omega_\nu \rightarrow -eV + i\delta}. \quad (\text{B7})$$

However, here we only comment that G_A is approximately proportional to G_T^2 and that under the Coulomb blockade condition G_A is renormalized by the phase fluctuation resulting in a value much smaller than G_T . Therefore when G_T is small as in the present treatment and assuming $G_A R_Q \ll 1$, we can neglect the influence of the finite G_A .

The Fourier transform of $h_{\text{tr}}(\tau)$ is given by

$$h_{\text{tr}}(i\varepsilon_n) = k_B T \sum_{\omega_s} h_0(i\varepsilon_n - i\omega_s) h_2(i\omega_s), \quad (\text{B8})$$

where $h_0(i\varepsilon_n)$ and $h_2(i\omega_s)$ are the Fourier transforms of $A_\psi(\tau)$ and $A_{\varphi_-}(\tau)$, respectively. From Eqs. (B2) and (B6), when $R_A \gg 1/(e\omega_g C_\Sigma)$,

$$h_0(i\varepsilon_n) = \frac{1 - e^{-4\beta E_C'(V_g)}}{4E_C'(V_g) - i\varepsilon_n}, \quad (\text{B9})$$

$$h_2(i\omega_n) = \beta \delta_{n,0}. \quad (\text{B10})$$

Then, finally

$$h_{\text{tr}}(i\varepsilon_n) = \frac{1 - e^{-4\beta E_C'(V_g)}}{4E_C'(V_g) - i\varepsilon_n}. \quad (\text{B11})$$

APPENDIX C: COOPERON IN QUASI-ONE-DIMENSIONAL LOOP STRUCTURE

For the quasi-one-dimensional loop structure illustrated in Fig. 11, the spatial variation of the cooperon is given as follows. We assume a unitary scattering matrix for the three branch nodes at $x = L_a, L_b$, as

$$S = \begin{bmatrix} 0 & 1/\sqrt{2} & 1/\sqrt{2} \\ 1/\sqrt{2} & -1/2 & 1/2 \\ 1/\sqrt{2} & 1/2 & -1/2 \end{bmatrix}, \quad (\text{C1})$$

where the first component corresponds to the left/right lead and the second and the third to the upper/lower arm of the loop. This assumption means the spatial derivative of the cooperon is conserved at the nodes, which means the conservation of the proximity current carried by the particle at the nodes. This is equivalent to the boundary condition for the quasiclassical Green's functions.³³

Using the scattering matrices and the boundary conditions at the both ends of the wire ($x = -L_S, L_N$), we solve the differential equation for cooperon Eq. (26) and get

$$C_p(x, x_0; z) = M_0(P e^{\kappa(z)(x-x_0)} + M_1 e^{-\kappa(z)(x-x_0)}), \quad (\text{C2})$$

for $x_0 < x < L_a$ (in the right lead), and

$$C_p(y_1, y_2; z) = M_e M_0 e^{[\kappa(z)+r]y_1} + M_f M_0 e^{-[\kappa(z)-r]y_1} + M_h M_0 e^{[\kappa(z)-r]y_2} + M_g M_0 e^{-[\kappa(z)+r]y_2}, \quad (\text{C3})$$

for $x_a < x < L_b$ (in the loop), and

$$C_p(x, x_0; z) = M_L M_0 \sinh[\kappa(z)(x - L_N)], \quad (\text{C4})$$

for $L_b < x < L_N$ (in the left lead), where

$$\kappa(z) = \sqrt{\frac{-2iz - 2\pi|n|k_B T}{D}}, \quad (\text{C5})$$

and

$$L_R = L_a - x_0, L_L = L_N - L_b \quad (\text{C6})$$

$$P = -e^{-2\kappa(z)(L_R + \pi R_0)} \{ \cos^2[r\pi R_0] (1 - e^{-2\kappa(z)\pi R_0}) e^{-2\kappa(z)L_R} + \sin^2[r\pi R_0] (1 - e^{-2\kappa(z)\pi(R_0 + L_L)}) \}, \quad (\text{C7})$$

$$M_1 = 1 - e^{-2\kappa(z)\pi R_0} (\cos^2[r\pi R_0] + \sin^2[r\pi R_0] e^{-2\kappa(z)L_L}), \quad (\text{C8})$$

$$M_0 = \frac{L_L + L_R + \pi R_0}{D\kappa(z)(M_1 - P)}, \quad (\text{C9})$$

$$M_f = \frac{1}{\sqrt{2}} \{1 - e^{-2\kappa(z)\pi R_0} e^{-ir\pi R_0} (\cos[r\pi R_0] - i \sin[r\pi R_0]) e^{-2\kappa(z)L_L}\} e^{-\kappa(z)L_R}, \quad (\text{C10})$$

$$M_g = \frac{1}{\sqrt{2}} \{1 - e^{-2\kappa(z)\pi R_0} e^{ir\pi R_0} (\cos[r\pi R_0] + i \sin[r\pi R_0]) e^{-2\kappa(z)L_L}\} e^{-\kappa(z)L_R}, \quad (\text{C11})$$

$$M_e = -\frac{1}{\sqrt{2}} e^{-\kappa(z)L_R} e^{-2\kappa(z)\pi R_0} e^{-ir\pi R_0} \{ \cos[r\pi R_0] \times (1 - e^{-2\kappa(z)\pi R_0}) e^{-2\kappa(z)L_L} + i \sin[r\pi R_0] \times (1 - e^{-2\kappa(z)(\pi R_0 + L_L)}) \}, \quad (\text{C12})$$

$$M_h = -\frac{1}{\sqrt{2}} e^{-\kappa(z)L_R} e^{-2\kappa(z)\pi R_0} e^{ir\pi R_0} \{ \cos[r\pi R_0] \times (1 - e^{-2\kappa(z)\pi R_0}) e^{-2\kappa(z)L_L} - i \sin[r\pi R_0] \times (1 - e^{-2\kappa(z)(\pi R_0 + L_L)}) \}, \quad (\text{C13})$$

$$M_L = -2 \cos[r\pi R_0] e^{-\kappa(z)(L_R + \pi R_0 + L_L)} (1 - e^{-2\kappa(z)\pi R_0}), \quad (\text{C14})$$

where

$$r = \frac{2}{R_0} \frac{\Phi}{\Phi_0}, \quad (\text{C15})$$

$\Phi_0 = h/e$, Φ is the magnetic flux piercing the ring. Similarly,

$$C_p(x, x_0; z) = \frac{L_C}{D\kappa(z)} \frac{\sinh[\kappa(z)|x|]}{\cosh[\kappa(z)L_c]} \quad (\text{C16})$$

for $-L_c < x < 0$ (in the lead right of the superconducting island).

-
- ¹B. Z. Spivak and D. E. Khmel'nitskii, Pis'ma Zh. Éksp. Teor. Fiz. **35**, 334 (1982) [JETP Lett. **35**, 412 (1982)].
- ²H. Nakano and H. Takayanagi, Solid State Commun. **80**, 997 (1991).
- ³H. Nakano and H. Takayanagi, Phys. Rev. B **47**, 7986 (1993).
- ⁴Yu. V. Nazarov and T. H. Stoof, Phys. Rev. Lett. **76**, 823 (1996).
- ⁵A. Volkov and H. Takayanagi, Phys. Rev. B **56**, 11 184 (1997).
- ⁶A. Volkov, N. Allsopp, and C. J. Lambert, J. Phys.: Condens. Matter **8**, L45 (1996).
- ⁷C. J. Lambert and R. Raimondi, J. Phys.: Condens. Matter **10**, 901 (1998).
- ⁸D. V. Averin and K. K. Likharev, in *Mesoscopic Phenomena in Solids*, edited by B. Altshuler, P. A. Lee, and R. A. Webb (Elsevier, Amsterdam, 1991).
- ⁹*Single Charge Tunneling*, Vol. 294 of *NATO Advanced Study Institute, Series B: Physics*, edited by H. Grabert and M. Devoret (Plenum, New York, 1992).
- ¹⁰G. Schön and A. D. Zaikin, Phys. Rep. **198**, 237 (1990).
- ¹¹C. Bruder, R. Fazio, and G. Schön, Phys. Rev. B **50**, 12 766 (1994).
- ¹²C. Bruder, R. Fazio, and G. Schön, Physica B **203**, 240 (1994).
- ¹³C. Bruder, R. Fazio, A. van Otterlo, and G. Schön, Physica B **203**, 247 (1994).
- ¹⁴A. I. Larkin and Yu. N. Ovchinnikov, in *Nonequilibrium Superconductivity*, edited by D. N. Langenberg and A. I. Larkin (North-Holland, Amsterdam, 1986), p. 493.
- ¹⁵J. Rammer and H. Smith, Rev. Mod. Phys. **58**, 323 (1986).
- ¹⁶R. Kubo, J. Phys. Soc. Jpn. **12**, 570 (1957).
- ¹⁷A. Huck, F. W. J. Hekking, and B. Kramer, Europhys. Lett. **41**, 201 (1998).
- ¹⁸F. W. J. Hekking and Yu. V. Nazarov, Phys. Rev. Lett. **71**, 1625 (1993).
- ¹⁹Yu. V. Nazarov, Phys. Rev. Lett. **73**, 1420 (1994).
- ²⁰A. V. Zaitsev, Phys. Lett. A **194**, 315 (1994).
- ²¹A. F. Volkov, A. V. Zaitsev, and T. M. Klapwijk, Physica C **210**, 21 (1992).
- ²²C. L. Kane, R. A. Serota, and P. A. Lee, Phys. Rev. B **37**, 6701 (1988).
- ²³V. Z. Kresin, Phys. Rev. B **34**, 7587 (1986).
- ²⁴Y. Takane and H. Ebisawa, J. Phys. Soc. Jpn. **61**, 3466 (1992).
- ²⁵K. Maki, Prog. Theor. Phys. **39**, 897 (1968); R. S. Thompson, Phys. Rev. B **1**, 327 (1970).
- ²⁶For example, see articles in *Electron-Electron Interactions in Disordered Systems*, edited by A. L. Efros and M. Pollak (North-Holland, Amsterdam, 1985).
- ²⁷For references, see articles in *Quantum Tunneling in Condensed Media*, edited by Yu. Kagan and A. J. Leggett (North-Holland, Amsterdam, 1992).
- ²⁸K. Awaka and H. Fukuyama, J. Phys. Soc. Jpn. **66**, 2820 (1997).
- ²⁹F. Guinea and G. Schön, Physica B **152**, 165 (1988).
- ³⁰H. Higurashi, S. Iwabuchi, and Y. Nagaoka, Phys. Rev. B **51**, 2387 (1995).
- ³¹N. Hatakenaka, J. Phys. Soc. Jpn. **67**, 3360 (1998).
- ³²H. Nakano and H. Takayanagi (unpublished).
- ³³A. V. Zaitsev, Zh. Éksp. Teor. Fiz. **59**, 896 (1994) [Sov. Phys. JETP **59**, 863 (1984)].